Construction and Building Materials 425 (2024) 136062

Contents lists available at ScienceDirect

Construction and Building Materials

journal homepage: www.elsevier.com/locate/conbuildmat

Integrating push-out test validation and fuzzy logic for bond strength study of fiber-reinforced self-compacting concrete

Vahid Shafaie [a], Oveys Ghodousian [b], Amin Ghodousian [c], Raffaele Cucuzza [d], Majid Movahedi Rad [a,*]

[a] Department of Structural and Geotechnical Engineering, Széchenyi István University, Győr 9026, Hungary
[b] Department of Civil Engineering, Takestan Branch, Islamic Azad University, Takestan, Iran
[c] Department of Engineering Science, University of Tehran, Tehran, Iran
[d] Department of Structural, Geotechnical and Building Engineering, Politecnico di Torino, Corso Duca degli 5 Abruzzi, 24, Turin, TO 10129, Italy

ARTICLE INFO

Keywords:
Fiber-reinforced Concrete
Self-compacting concrete
Shear bond strength
Push-out test
Fuzzy logic
Pozzolan

ABSTRACT

This study offers a comprehensive analysis of Fiber-Reinforced Self-Compacting Concrete (FRSCC) with a focus on shear bond strength influenced by specific compositions of microsilica, zeolite, slag, and polypropylene fibers. Twenty distinct FRSCC mixes underwent extensive testing, including 28-day compressive strength, tensile strength assessments, and push-out and slant shear tests. A significant outcome is the strong correlation between the push-out and slant shear test results, exemplified by an R^2 value of 0.88, confirming the push-out test as a viable and practical alternative for bond strength assessment. Experimentally, fibers were found to enhance tensile strength, with the inclusion of 15% microsilica and slag further amplifying this effect, highlighting the critical role of precise pozzolan selection in achieving optimal mechanical performance and workability in FRSCC. Furthermore, the study introduces a fuzzy logic system for predicting shear bond strength, achieving high predictive accuracy with R^2 values reaching up to 0.96, depending on the t-norms utilized. This research not only validates the push-out test as a reliable method for evaluating shear bond strength in FRSCC but also demonstrates the efficacy of the fuzzy logic approach, representing a groundbreaking contribution in both computational analysis and practical methodology for concrete structural integrity.

1. Introduction

The deterioration of existing concrete structures necessitates significant attention towards maintenance, repair, and reinforcement activities. Cementitious materials, such as mortar or concrete, are widely employed in rehabilitating bridges and buildings. A common approach in these processes is the addition of a thin layer of concrete, varying in thickness from 20 to 100 millimeters, which may be used independently or reinforced with steel bars, metallic, or synthetic fibers. The application of cementitious materials in structural strengthening is exemplified by patching or replacing concrete overlays on floors or decks and using structural concrete jacketing for columns. Generally, in the construction of concrete structures, it is customary to cast concrete at different times, both in structures still under construction and in existing structures, as a new element or as a repair layer for strengthening. Various methodologies are employed to evaluate the bond strength of new-to-old concrete, including splitting [1], pull-off [2], slant shear [3–11], twist-off, and friction transfer techniques [12]. The selection of materials and rigorous quality control are imperative for ensuring a repair layer that is not only appropriate but also durable and cost-effective. A key characteristic of a successful repair layer is its high adhesion to the concrete substrate [13]. While a substantial body of research focused on the bond strength between traditional vibrated concrete used in both old and new contexts [14–16], studies examining the behavior of self-compacting concrete as an overlay on concrete substrates are comparatively limited [17,18]. Among the various tests for evaluating bond strength between concrete layers, the slant shear test is notably the most widely utilized [19].

The occurrence of cracks in the repair layer is a critical concern, as it significantly impacts the structural functionality of the layer. This includes aspects such as tensile strength, shear and flexural stiffness, energy absorption capacity, durability, bonding to the substrate layer, and resistance to reinforcement corrosion [20]. Moreover, cracking in the repair layer facilitates the penetration of deleterious materials into the

* Corresponding author.
E-mail address: majidmr@sze.hu (M. Movahedi Rad).

https://doi.org/10.1016/j.conbuildmat.2024.136062
Received 1 February 2024; Received in revised form 3 March 2024; Accepted 27 March 2024
Available online 1 April 2024

interface between the substrate and the repair layer. This not only increases vulnerability but also leads to early saturation of the repair layer, contributing to damage from freeze-thaw cycles, salt absorption, and, ultimately, structural failure [21]. A viable strategy for mitigating cracking in concrete involves using various fibers, such as steel, carbon, and polypropylene, which are randomly integrated within the concrete matrix [22,23]. These fibers effectively prevent crack propagation by forming bridging actions across the developing cracks. This mechanism not only influences the length and width of shrinkage cracks but also diminishes damage at the interface, consequently enhancing the bond strength between the concrete layers. Furthermore, the incorporation of fibers significantly improves the mechanical properties of the repair layer, including its durability, toughness, impact resistance, and fatigue strength, which are beneficial attributes.

Recent research in fiber-reinforced concrete has demonstrated significant advancements in the strength and ductility of reinforced structures, particularly with the incorporation of hybrid steel and polypropylene fibers, which aligns well with the focus on enhancing the mechanical properties of repair layers. This emphasis on hybrid fiber compositions is crucial for improving the overall performance of concrete in structural applications, underscoring the vital role of fiber integration in developing more resilient and durable concrete technologies [24]. Alongside advancements in hybrid fiber compositions, the exploration of carbon fiber-reinforced polymers in concrete technology underscores the growing recognition of fibers' critical role in enhancing structural resilience and performance [25]. While fibers contribute positively to these aspects, it is noteworthy that steel rebars, in contrast, are capable of transferring substantially greater forces. However, the use of steel rebars is contingent upon the repair layer being sufficiently thick. An additional benefit of employing fibers is their contribution to reducing the risk of corrosion. In scenarios where the repair layer comprises cementitious materials with a considerable thickness (exceeding 25 mm), it is observed that the maximum shear and tensile stresses are relatively comparable [21]. Moreover, fibers are known to enhance the overall mechanical properties of concrete, such as its durability, toughness, and resistance to both impact and fatigue [26].

Numerous studies have explored the impact of fibers on the behavior of concrete overlays and their adhesion to underlying concrete substrates [27–31]. In France, a decade-long investigation into the interplay between shrinkage and debonding in repair layers affirmed the beneficial influence of fiber reinforcement [32]. Additionally, it has been observed that fiber-reinforced cementitious repair layers exhibit a lower susceptibility to fatigue when compared to their non-fiber counterparts [33,34]. Feng et al. [35] undertook a comprehensive evaluation of the bond strength between ultra-high-performance concrete (UHPC) and conventional strength concrete, employing slant shear and direct tensile tests to assess bonding. Their findings indicated that the direct tensile bond strength displayed a higher coefficient of variation compared to that obtained through the modified direct tensile test method. Diab et al. [19] conducted research on the bond strength between aged and newly cast self-compacting concrete, utilizing the slant shear method. Their results showed a significant slant shear bond strength enhancement by incorporating polypropylene fibers. Hu et al. [36] embarked on an experimental investigation to evaluate the dynamic slant shear bond behavior between new and old concrete, demonstrating that strain rate plays a crucial role in determining failure modes and bond strength. Saldanha et al. [37] developed a modified slant shear test designed to consistently induce adhesive failures (interface debonding) under various conditions, substantiated through numerical and experimental testing. Further, Feng et al. [38] assessed the bond properties of UHPC and normal concrete through slant shear tests involving different slant angles and splitting strength tests. They concluded that the combination of UHPC with high-pressure water treatment of the substrate surface results in effective repair. In another study, Feng et al. [39] investigated how factors such as fiber stiffness, the surface roughness of the substrate, and surface angle affect the bond strength between a concrete substrate and repair mortar. Their findings highlighted that increased roughness enhances bond strength, and that steel fibers improve adhesion more effectively compared to carbon fibers. Zanotti et al. [14] analyzed various test series to determine the interface bond strength between concretes of different ages, finding that test geometry significantly influences failure modes, stress paths, and bond strength values. Luo et al. [40] utilized a finite element model to optimize the interfacial relationship by adjusting groove configurations. Ghodousian et al. [2] explored the bonding of self-compacting concrete containing mineral pigments to concrete substrates, using pull-off and push-out methods. Their research indicated that the push-out method is particularly reliable for assessing the bond strength between two concrete layers. In another application, Ghodousian et al. [41] successfully employed the push-out method to determine the bonding efficiency of facade stones to concrete substrates.

In recent decades, a myriad of studies have leveraged soft computing techniques to forecast various characteristics of concrete. These include artificial neural networks [42–48], algorithms inspired by nature [49], and fuzzy logic systems [12,46–48,50–54]. For instance, Silva et al. [55] adeptly merged fuzzy logic with genetic algorithms to predict the shrinkage behavior of concrete. Arslan et al. [56] employed a rule-based Mamdani type fuzzy logic model to estimate the bond behavior of lightweight concrete. In their study, Najjar et al. [57] utilized fuzzy logic systems to forecast the engineering properties of pre-placed aggregate concrete, demonstrating that such models are beneficial tools in the design process of these mixes. Rashid et al. [58] applied fuzzy logic systems to predict the compressive strength of concrete containing green foundry sand. Beycioglu et al.[59] developed a similar rule-based Mamdani type fuzzy logic model to predict the mechanical properties of blended cement under elevated temperatures. Among these various mathematical approaches, fuzzy systems have shown particular efficacy in calculating the fresh properties of fiber-reinforced concrete [60]. This success underscores the potential of soft computing methods in enhancing our understanding and prediction of concrete properties, providing valuable insights for both research and practical applications in the field of concrete technology.

This research primarily aims to validate the push-out test as a reliable and simpler alternative to the slant shear test for assessing the shear bond strength of the repair layer in self-compacting concrete (SCC). The slant shear test, while offering valuable insights, has a significant drawback in that it can result in two different failure modes: adhesive failure at the interface or cohesive failure within the monolithic material. Particularly in cases of rough interfaces, a cohesive failure may only provide a lower estimate of the actual interface strength, obscuring the true bond characteristics[37]. This limitation underscores the importance of the push-out test as a more reliable method for evaluating shear bond strength, especially in scenarios where distinguishing between the interface and material strength is crucial. In addition to the core focus on shear bond strength tests, the study also conducts comprehensive 28-day compressive strength, splitting tensile strength, and slump flow tests to investigate the effects of the utilized pozzolans and fibers on these fundamental properties. The study meticulously investigates the bond strength of SCC, integrating micro silica, zeolite, and slag in varying proportions of 5, 10, and 15% by weight of cement, and examines the effects of polypropylene fibers at dosages of 0 and 0.1% by volume. In the course of this study, both slant shear and push-out tests were utilized to assess bond strength. The observed substantial correlation between these methodologies underscores the push-out test's potential as a more expedient and practical option compared to the slant shear test for evaluating shear bond strength. The study also introduces a pioneering method to bolster this experimental approach to predict the bond strength between fiber-reinforced SCC (FRSCC) and normal concrete under shear force using a fuzzy system. This system, equipped with a generalized Mamdani's interference engine and the Frank family of t-norms, aims to offer more precise and robust predictions of bond strength. The adoption of a fuzzy logic system is particularly

advantageous due to its capability to model the uncertain and complex nature of bond strength in FRSCC, providing a more accurate and reliable predictive tool. This integration of advanced fuzzy logic not only validates the experimental findings but also enhances the predictability of bond strength, thereby contributing to the field of concrete technology with a focus on practical and efficient testing methods.

2. Materials and methods

This section outlines the experimental and predictive methodologies employed to assess the shear bond strength of FRSCC. Assessment techniques include slant shear and push-out tests, complemented by predictive models based on linear regression and a proposed generalized Mamdani fuzzy system. The methodology process depicted in Fig. 1 comprises two main stages: conducting laboratory experiments to measure shear bond strength and employing predictive methods to analyze and interpret these data.

2.1. Mix proportions and materials properties

Table 1 comprehensively summarizes the twenty mixtures formulated in this research. For all FRSCC mix designs in this study, the fine aggregate component consisted exclusively of river sand, characterized by a maximal particle size of 3.0 mm, an apparent specific gravity of 2700 kg/m^3, and a water absorption capacity of 1.5%. The coarse aggregate used had a maximal size of 12.5 mm [61]. Cementitious material selection was uniform across all mixes, utilizing Cement type CEMI 42.5. The study utilized three distinct types of pozzolans: Microsilica (MS), Zeolite (ZE), and Slag (SL). These were incorporated in proportions of 0, 5, 10, and 15 percent by weight of cement. A detailed insight into the cement and pozzolans' physical properties and chemical compositions can be found in Table 2, while Fig. 2 visually showcases these three distinct pozzolans used in the FRSCC mixes.

Normal tap water was employed as the mixing water in all FRSCC batches. The proportion of superplasticizers added was consistently set at 1.1% of the total weight of the cementitious components. Polypropylene fibers were included in the mixtures at two levels: 0 and 0.1 percent by volume, following the optimized dosage of 0.1% as recommended for achieving the best balance between mechanical properties and volume fractions [62,63]; the properties of these fibers are detailed in Table 3, while Fig. 2 illustrates the polypropylene fibers.

2.2. Testing procedures

2.2.1. Slump flow, Compressive and Tensile Strength

Upon preparation of each mix, the slump flow test was initially conducted in its fresh state. It is pertinent to note that, for this study, the criterion for considering the mixes as self-compacting was established at a slump flow of 550 mm. This benchmark, while slightly below the 600 mm limit set by guidelines such as EFNARC [64], aligns with other standards [65,66] that stipulate a 550 mm threshold. Following the slump flow assessment, the mixtures were methodically cast into 15 cm cubic molds designated for the 28-day compressive strength test and into standard cylindrical molds for the Brazilian test (Fig. 3). These tests adhered to the guidelines set by ASTM C39 [67].

2.2.2. Shear bond Strength

Both push-out and slant shear methods were employed to evaluate the bonding of the mixtures when used as a repair layer on concrete substrates. The slant shear test is designed to exert a compressive load on a cylindrical specimen composed of repair material and substrate joined at a fixed 30-degree angle. This configuration induces a combination of shear and normal stresses along the interface between the substrate and the repair material. In the preparation of these composite specimens, the concrete substrate was cast initially. Half-molds were utilized to form only one portion of the ultimate specimen. Post-casting, the samples were immediately covered with plastic sheets, demolded after 24 hours, and then subjected to standard curing conditions in a moisture and temperature-controlled environment. Subsequently, the concrete halves were allowed to air-dry for a period of 24 hours. The final step involved pouring the new mortar onto the substrates in an optimal Saturated Surface Dry (SSD) state, followed by curing per the plain concrete pro-

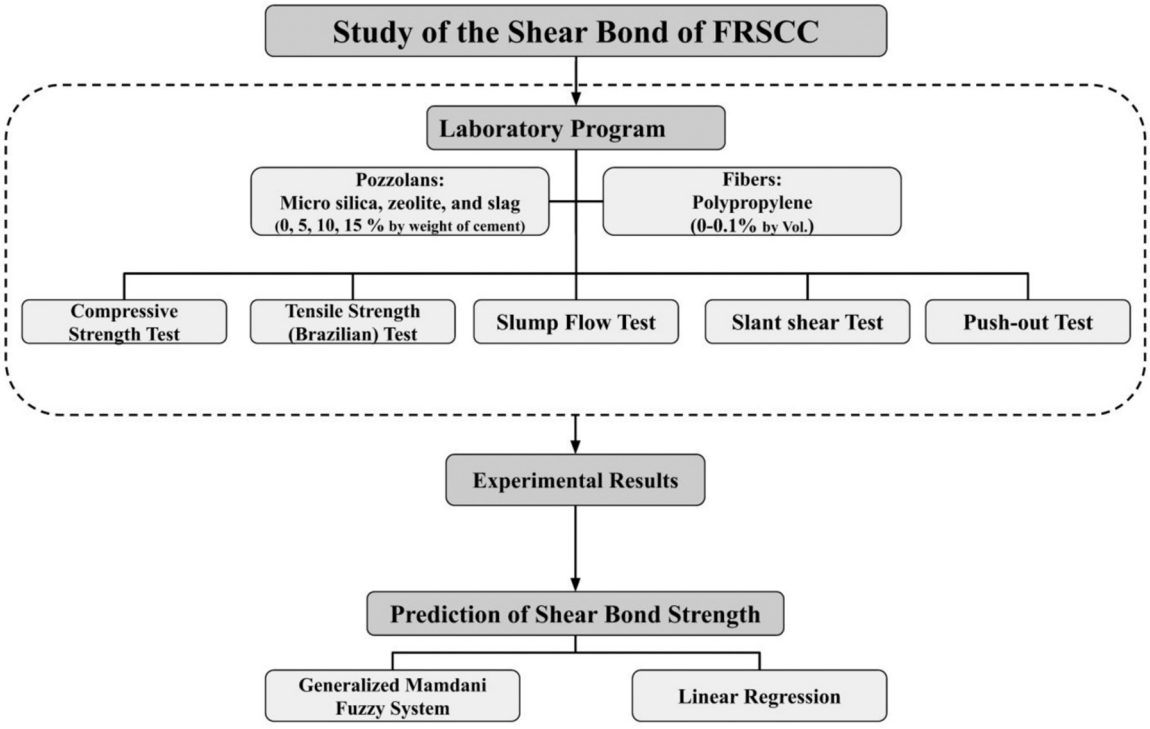

Fig. 1. Schematic representation of methodological approach.

Table 1
Mix proportions used in this study.

No.	Mix ID	Cement	Pozzolan			Limestone	Sand	Gravel	Water	W/P*	PP**	SP***
		Kg/m^3	**Type**	**%**	**Kg/m^3**	**Kg/m^3**	**Kg/m^3**	**Kg/m^3**	**Kg/m^3**		**%**	**%**
1	CTRL	500	—	0	0	277	793	691	180	0.36	0	1.1
2	MS5	475	Microsilica	5	25	277	793	691	180	0.36	0	1.1
3	MS10	450	Microsilica	10	50	277	793	691	180	0.36	0	1.1
4	MS15	425	Microsilica	15	75	277	793	691	180	0.36	0	1.1
5	ZE5	475	Zeolite	5	25	277	793	691	180	0.36	0	1.1
6	ZE10	450	Zeolite	10	50	277	793	691	180	0.36	0	1.1
7	ZE15	425	Zeolite	15	75	277	793	691	180	0.36	0	1.1
8	SL5	475	Slag	5	25	277	793	691	180	0.36	0	1.1
9	SL10	450	Slag	10	50	277	793	691	180	0.36	0	1.1
10	SL15	425	Slag	15	75	277	793	691	180	0.36	0	1.1
11	CTRL-F	500	—	0	0	277	793	691	180	0.36	0.1	1.1
12	MS5F	475	Microsilica	5	25	277	793	691	180	0.36	0.1	1.1
13	MS10-F	450	Microsilica	10	50	277	793	691	180	0.36	0.1	1.1
14	MS15-F	425	Microsilica	15	75	277	793	691	180	0.36	0.1	1.1
15	ZE5-F	475	Zeolite	5	25	277	793	691	180	0.36	0.1	1.1
16	ZE10-F	450	Zeolite	10	50	277	793	691	180	0.36	0.1	1.1
17	ZE15-F	425	Zeolite	15	75	277	793	691	180	0.36	0.1	1.1
18	SL5-F	475	Slag	5	25	277	793	691	180	0.36	0.1	1.1
19	SL10-F	450	Slag	10	50	277	793	691	180	0.36	0.1	1.1
20	SL15-F	425	Slag	15	75	277	793	691	180	0.36	0.1	1.1

(* Water to powder (cement + pozzolan) ratio; ** Polypropylene fiber; *** Super plasticizer)

Table 2
Physical properties and Chemical composition of utilized cement and three pozzolans.

Properties	Cement	ZE	MS	SL
Physical Properties				
Specific Gravity (g/cm^3)	3.15	2.37	2.25	2.89
Bulk Unit Weight (g/cm^3)	1.40	0.77	0.25	1.22
Specific Surface Area (cm^2/g)	2910	3450	200,000	4600
Color	Gray	Pale Beige	Dark Bluish-Gray	Off-White
Chemical composition (%)				
CaO	21.32	1.68	0.10–0.70	40.60
SiO2	4.81	67.79	86–94	33.10
Al2O3	3.83	13.66	0.20–2.00	13.70
Fe2O3	62.85	1.44	0.20–2.50	3.12
MgO	1.48	1.20	0.30–3.50	8.70
K2O	2.32	1.42	0.50–3.00	0.16
Na2O	0.47	2.04	0.20–1.50	0.07
SO3	0.69	0.50	0.10–0.30	0.60
L.O.I	2.04	10.23	2.10	0.04

Fig. 2. Polypropylene fiber (P.P), Zeolite (ZE), Micro Silica (MS) and SLag used in FRSCC mixes.

tocol (Fig. 4-a). The substrate-repair interfacial stresses for the slant shear test are illustrated in Fig. 4-b:

$$\tau_n = \frac{\sigma_0 \sin(2\alpha)}{2} \quad (1)$$

$$\sigma_n = \sigma_0 \quad (\sin\sigma)^2 \quad (2)$$

In this context, τ_n represents the shear stress acting parallel to the bond plane, whereas σ_0 is the applied axial stress that fails the bond plane. Additionally, σ_n denotes the normal stress acting perpendicular to the bond plane.

The Mohr-Coulomb criterion is widely recognized and employed to characterize the shear bond strength in relation to the normal interfacial stresses and intrinsic interfacial properties. This methodological approach is also endorsed and utilized within various design codes [1], underscoring its relevance and applicability in the analysis and design processes pertaining to the shear bond strength of materials.

$$\tau_n = C + \sigma_n \quad \tan(\varphi) \quad (3)$$

Whereas, C represents the adhesion strength, often referred to as cohesion, and φdenotes the internal angle of friction. These parameters are fundamental in defining the interfacial shear strength. In addition, Fig. 4-c illustrates a specimen post-failure, providing a visual reference to the outcome of the applied stress and the resultant fracture pattern as per the Mohr-Coulomb failure criterion.

The push-out test is designed to assess the adhesion between two concrete layers under direct shear conditions, effectively isolating the adhesion effect from any frictional contribution through compression loading on a cylindrical specimen. In contrast, the slant shear test facilitates the evaluation of both adhesion and friction forces, resulting in a more evenly distributed shear-induced stress along the interface. For these experiments, the substrate comprised two concrete blocks, each 5 cm thick, extracted from cubes cast six months before testing. Sandwiched between these blocks was a 5 cm block cast with the SCC mixes, thereby creating a composite 15 cm cube (as illustrated in Fig. 5-a). This arrangement ensured that the SCC repair layer was bonded to the

Table 3
Properties of polypropylene fibers used in FRSCC mixes.

Polypropylene	Specific gravity	Elongation at rupture	Absorption	Melting point	Length	Tensile strength
	900 kg/m^3	500%	Nil	175°C	12 mm	33. Pa

Fig. 3. Tests on FRSCC mixes (a) slump flow, (b) compressive strength, (c) tensile strength.

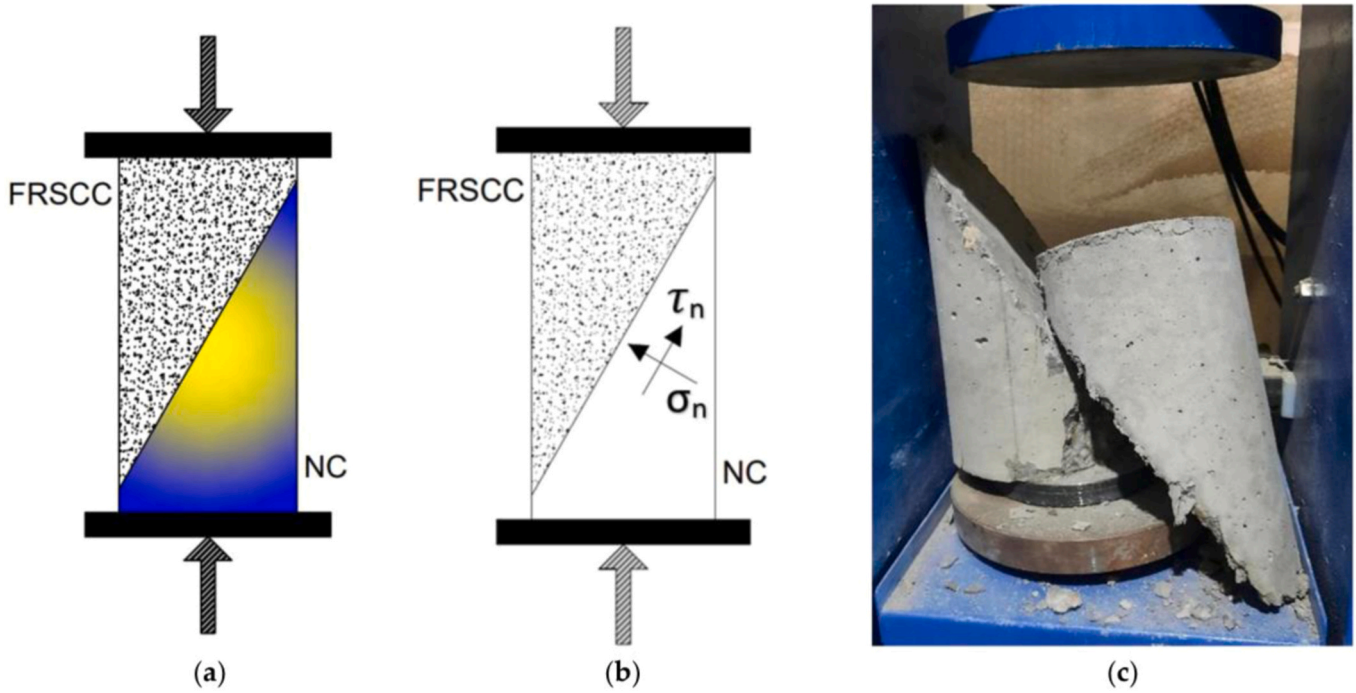

Fig. 4. (a) Schematic figure of slant shear test, **(b)** Normal and shear stresses at the interfacial in the slant shear test, **(c)** Typical failure of the slant shear test; NC=normal concrete.

substrate on two faces. Typically, failure in these tests occurs at the interface with the weakest bond strength. It is essential to highlight that for the push-out specimens, the concrete substrate was in an SSD state at the time of casting the SCC repair layer, as this condition is optimal for enhancing the interfacial bond. Fig. 5-b depicts a typical specimen post-failure.

2.3. Background on Generalized Mamdani's Fuzzy System

The design of the fuzzy system in this study was approached through a three-step algorithm. Consider a set of N input-output pairs$(x^1,y^1),(x^2,y^2),\ldots,(x^N,y^N)$ are given, where $x^k = (x_1^k, \ldots, x_n^k), \forall k \in \{1, \ldots, N\}$, i.e., $\mathscr{X}^{\mathscr{K}} \in U = U_{1\times}U_{2\times\ldots\times}U_{\prime\prime} \subseteq \mathscr{R}^{\prime\prime}$ and $\gamma^K \epsilon \quad V \subseteq \mathscr{R}$. The goal is to construct a fuzzy system $f(x)$ based on M input-output pairs (training phase). The process involves the following steps:

Step 1. Define fuzzy sets to cover the input and output spaces.

In this step, for each U_j $(j = 1,\ldots,n)$, M fuzzy sets A_j^l $(l = 1,\ldots,M)$ are defined. These sets must be completed within U_j, meaning for any $x_j \in U_j$, there exists a set A_j^l such that the membership function $\mu_{A_j^l}(x_j) \neq 0$. As an illustration, by defining $\mu_{A_j^l}(x_j)$ as a Gaussian membership function (Eq. (4)), it may be considered that $\sigma_j^l = \left|\overline{x}_j^{(l+1)} - \overline{x}_j^l\right|/2$ $(l = 1, 2, \ldots, M)$:

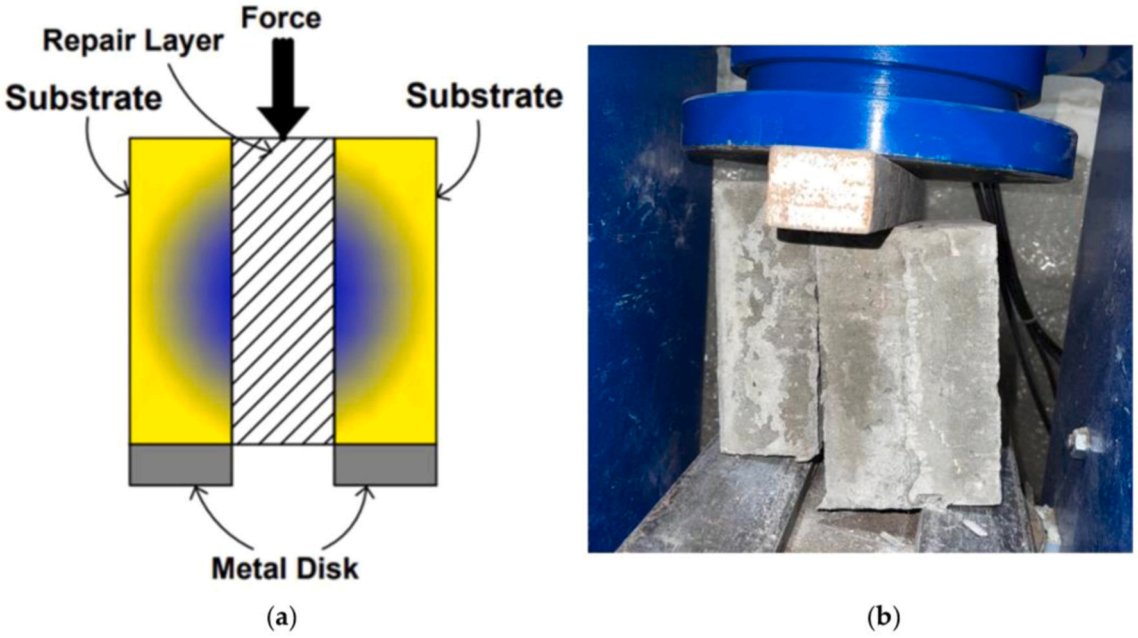

Fig. 5. (a) Schematic figure of the push-out test, (b) Typical failure of the push-out test.

$$\mu_{A_j^l}(x_j) = e^{-\left(\frac{x_j-\bar{x}_j^l}{\sigma_j^l}\right)^2} \quad (4)$$

where $\bar{x}_j^l$ is the center of the individual fuzzy set A_j^l; and $\sigma_j^l > 0$.

Step 2. Create the fuzzy rule base.

The second step of the algorithm is dedicated to generating a fuzzy rule base. For each input-output pair, represented as $(x^l, y^l) = (x_1^l, \ldots, x_n^l, y^l)$, where $l = 1, 2, \ldots, M$, the algorithm constructs an individual IF-THEN rule. The structure of these rules is defined as follows:

$$Rule(l): IF(x_1^l is A_1^l) and (x_2^l is A_2^l) and \ldots and (x_n^l is A_n^l), THEN(y^l is B^l) \quad (5)$$

where A_i^l and B^l $(l = 1, 2, \ldots, M)$ are fuzzy sets in $U_i \subseteq \mathscr{R}$ $(i = 1, 2, \ldots, n)$; and $V \subseteq \mathscr{R}$. Additionally, $x = (x_1, x_2, \ldots, x_n)^T \in U$ and $y \in V$ are the input and output variables of the fuzzy system, respectively, where $U = U_1 \times U_2 \times \ldots \times U_n \subseteq \mathscr{R}^n$. The fuzzy implications of these rules translate the fuzzy IF-THEN rule into a fuzzy relationship within the combined input-output product space $U \times V$.

Step 3. Construct the fuzzy system based on the fuzzy rule base.

The final step involves the construction of the fuzzy system utilizing the rule base established in Step 2. This is achieved by applying Eq. (6), which integrates the rules into a comprehensive fuzzy system:

$$f(x) = \frac{\sum_{l=1}^{M} \bar{y}^l \varphi_{j=1}^n (\mu_{A_j^l}(x_j))}{\sum_{l=1}^{M} \varphi_{j=1}^n (\mu_{A_j^l}(x_j))} \quad (6)$$

In this equation, $x \in U \subseteq \mathscr{R}^n$ represents the input to the fuzzy system; and $\mathscr{F}(x) \in V \subseteq \mathscr{R}$ denotes the output or the desired approximator of the fuzzy system.

3. Results and discussion

3.1. Experimental Results

The results of the 28-day compressive strength, splitting tensile strength, slump flow, and shear strength tests (push-out and slant shear) are systematically listed in Table 4. Specifically, for the slant shear test, the interfacial shear and normal stresses were calculated using Eqs. (1) and (2), offering a quantified assessment of the adhesion properties and integrity of the concrete interface.

Table 4
Tests results.

Mix ID	Slump Flow (cm)	Compressive strength (MPa)	Tensile strength (MPa)	Push-out bond strength (MPa)	Slant shear bond strength (shear stress) (MPa)
CTRL	66	53.21	4.09	1.54	8.72
MS5	69	57.01	4.48	2.04	10.87
MS10	73	62.34	4.69	2.16	14.59
MS15	73	59.75	4.66	2.1	14.31
ZE5	65	54.03	4.15	1.93	11.44
ZE10	63	50.29	4	1.8	9.87
ZE15	60	47.23	3.74	1.71	9.81
SL5	68	56.62	4.42	1.95	12.03
SL10	71	55.32	4.4	1.83	11.89
SL15	72	51.09	4.16	1.72	11.55
CTRLF	62	53.31	4.54	1.91	12.1
MS5F	66	57.72	5.04	2.28	14.24
MS10F	70	63.6	5.64	2.68	17.1
MS15F	70	59.43	5.16	2.64	16.18
ZE5F	63	53.89	4.97	2.14	13.12
ZE10F	60	50.23	4.55	2.09	12.97
ZE15F	55	47.63	4.39	1.93	12.03
SL5F	64	57.51	5.09	2.38	13.5
SL10F	68	54.22	4.78	2.25	13.14
SL15F	70	50.92	4.55	2.15	12.79

3.1.1. Slump flow, compressive, and tensile strength

The slump flow test outcomes presented in Fig. 6 provide a detailed examination of how fibers and various pozzolanic additives influence the workability of both SCC and FRSCC mixes. The standard SCC mix (CTRL) showcases a slump flow of 66 cm, demonstrating high inherent workability. Upon the introduction of fibers, as seen in the FRSCC control mix (CTRLF), workability slightly diminishes to 62 cm, evidencing the fibers' tendency to reduce flowability. However, the introduction of microsilica in FRSCC mixes, especially notable in MS10F and MS15F with slump flows of 70 cm each, suggests that microsilica can enhance workability, potentially offsetting the fibers' reducing

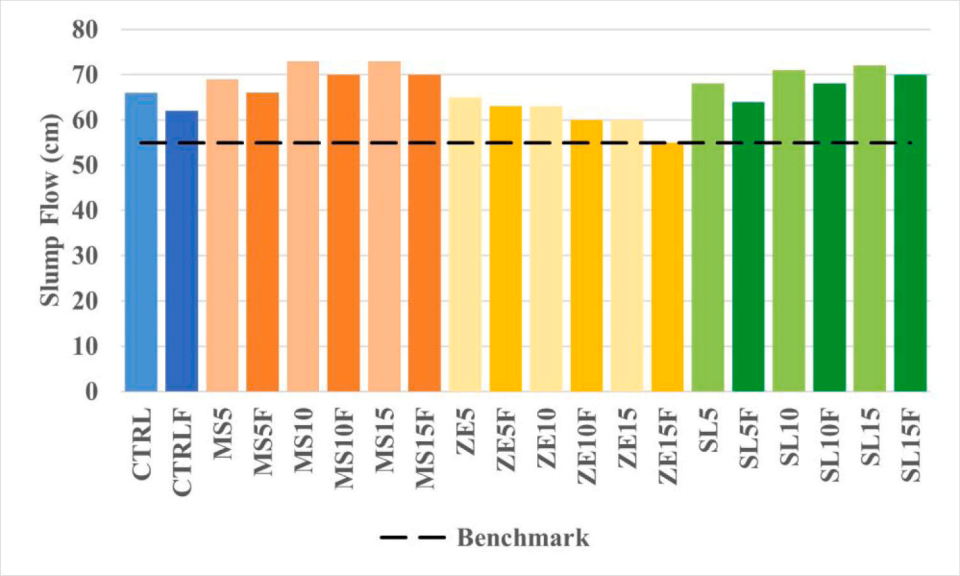

Fig. 6. Slump flow results of the SCC and FRSCC mixes.

effect. In contrast, zeolite and slag containing FRSCC mixes, while showing a decrement in workability with ZE15F at the benchmark of 55 cm and SL mixes like SL15F maintaining higher slump flows at 70 cm, indicate a more complex interaction between fibers and these pozzolans, where slag appears to have a lesser impact on reducing workability compared to zeolite. This layered analysis underscores that while fibers generally lessen the flowability of SCC, the judicious integration of pozzolans like microsilica can counterbalance this effect (The reason for this issue can be related to the finer particles of pozzolans compared to cement. This makes the mixture of water and powdered materials more paste-like and smoother.), ensuring the retention of self-compacting properties across both SCC and FRSCC formulations.

Compressive strength characteristics, presented in Fig. 7, indicate a marginal difference between SCC and FRSCC, suggesting that the primary role of fibers may not be in the enhancement of compressive strength. Instead, the significant role of pozzolanic materials, especially micro silica at optimal dosages, is highlighted in the improvement of compressive strength, since pozzolans such as microsilica provide more uniform distribution and greater volume of hydration products. Besides, as a filler they reduce the average pore size of cement paste. The peak strength exhibited by mixes with a 10% inclusion of microsilica underscores its efficacy in refining the microstructural attributes of SCC while contributing to the adhesion properties noted earlier.

As depicted in Fig. 8, the tensile strengths of FRSCC variants exhibit significant enhancements, reinforcing the assertion that fibers play a crucial role in augmenting tensile performance. The fibers' intrinsic ability to interlace through and bridge cracks substantiates their inclusion in SCC, particularly in applications where resistance to tensile stress is imperative. Moreover, the synergy between the pozzolanic materials and the fibers is evident, with microsilica imparting the most substantial improvement in tensile strength. While zeolite shows a less pronounced enhancement, the combination of 15% microsilica emerges as particularly efficacious. In the case of slag, its positive influence becomes most noticeable at a 15% inclusion level, suggesting a favorable interaction with fibers in bolstering tensile strength. This data highlights the nuanced role of pozzolanic proportions in achieving optimal tensile

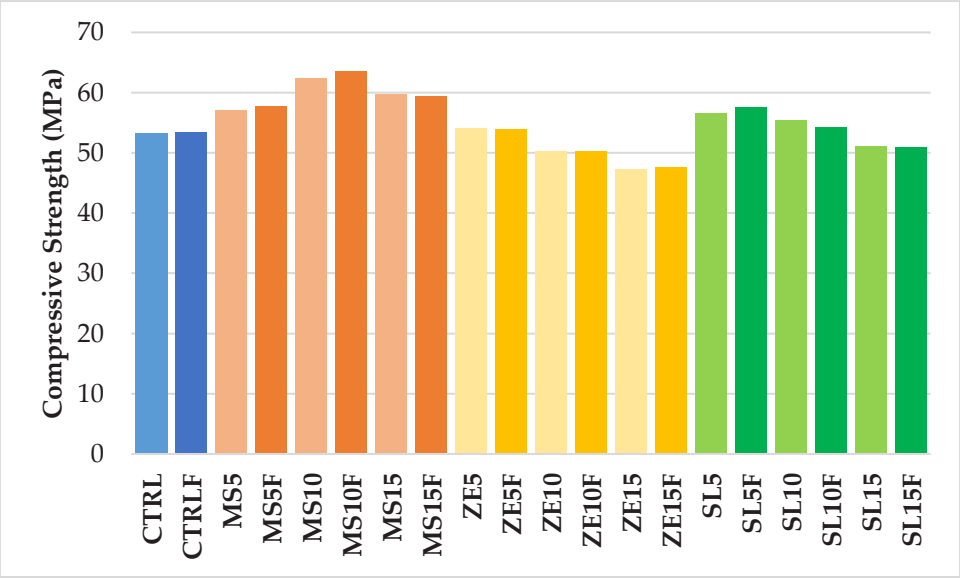

Fig. 7. Compressive strength results of the SCC and FRSCC mixes.

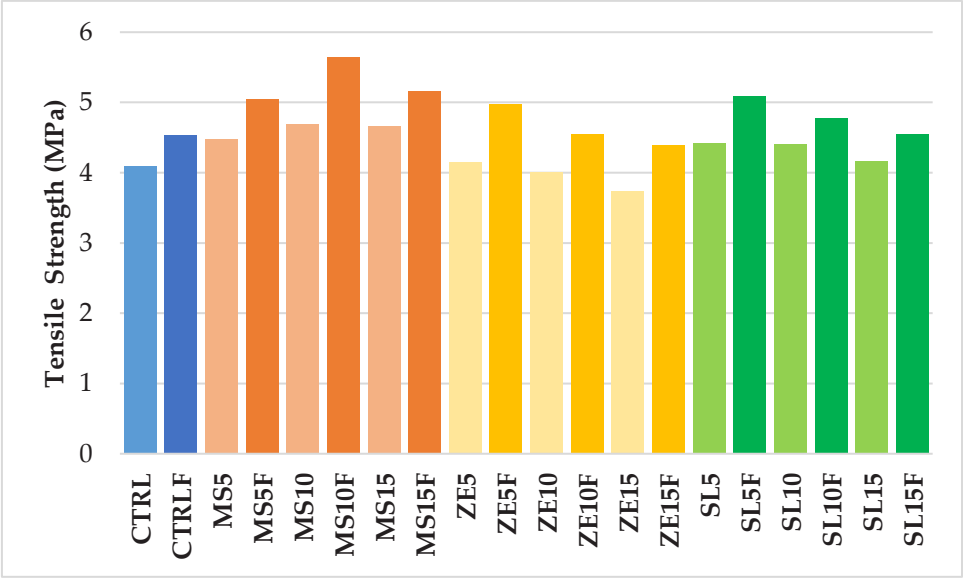

Fig. 8. Tensile strength results of the SCC and FRSCC mixes.

enhancement and underscores the necessity of deliberate pozzolan selection to synergize with fiber benefits, thereby optimizing mechanical properties and bond strength for repair applications.

3.1.2. Shear bond strength

The core of this study centers on the shear bond strength, specifically examining the push-out shear bond strength of FRSCC repair layers as compared to a standard SCC mix, which is pivotal to the structural integrity and durability of concrete infrastructures. Fig. 9 delineates the percentage change in push-out shear bond strength when FRSCC repair layers with polypropylene fibers are bonded to concrete substrates, in comparison to the control mix. The data indicate that the incorporation of fibers generally enhances bond strength, yet the degree of improvement varies significantly with different additives. Specimens with 5–15% microsilica content exhibit a diverse impact on bond strength, with an optimal 15% mix achieving a 25.71% increase, suggesting a nonlinear response to microsilica addition. Zeolite mixes demonstrate a progressive decrease in bond strength enhancement, with the highest zeolite content mix (ZE15F) only yielding a 12.87% increase, possibly due to the mix's reduced workability affecting fiber distribution and bond effectiveness. In contrast, slag mixes show a promising trend, with the bond strength incrementally improving with higher slag content, peaking at a 25% increase for the 15% slag mix (SL15F), indicative of a favorable synergy between slag and fibers in the bond strength matrix. This increase can probably be attributed to the less shrinkage of the repair layer containing slag and fibers, which reduces the stresses at the interface and therefore increases the bond strength between the two concrete layers.

Fig. 10 depicts the correlation between shear stress as determined by the slant shear and push-out tests. The R^2 value of 0.88 suggests a strong correlation between these two testing methods. Consequently, given the satisfactory results obtained from the push-out test, this method was selected for use in the finite element model. The push-out test offers several advantages over the slant shear method, particularly in terms of

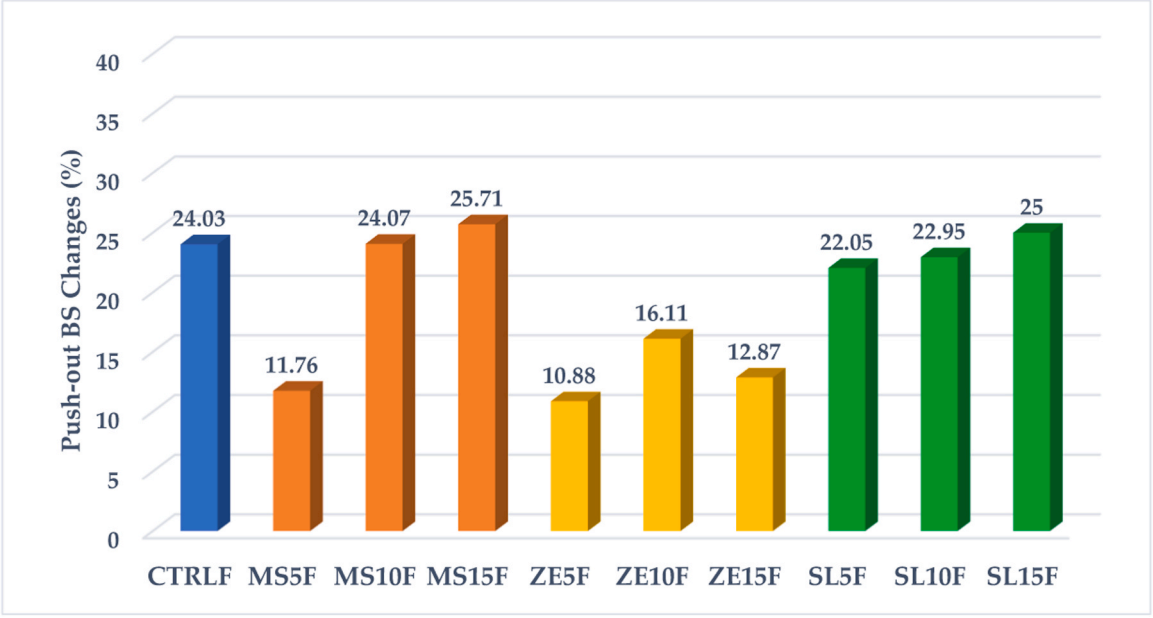

Fig. 9. Push-out bond strength changes attributable to the presence of fibers.

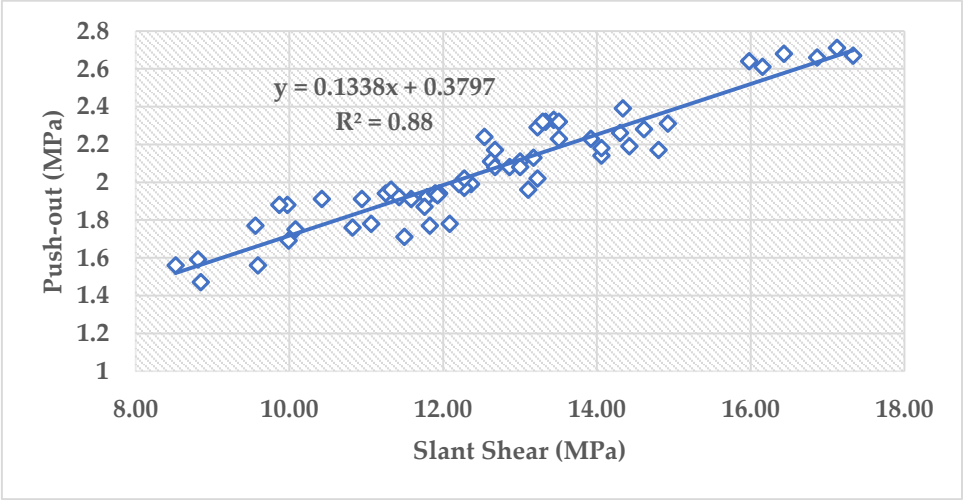

Fig. 10. Correlation of Shear Bond Stress (SBS) derived from Slant Shear and Push-out Tests.

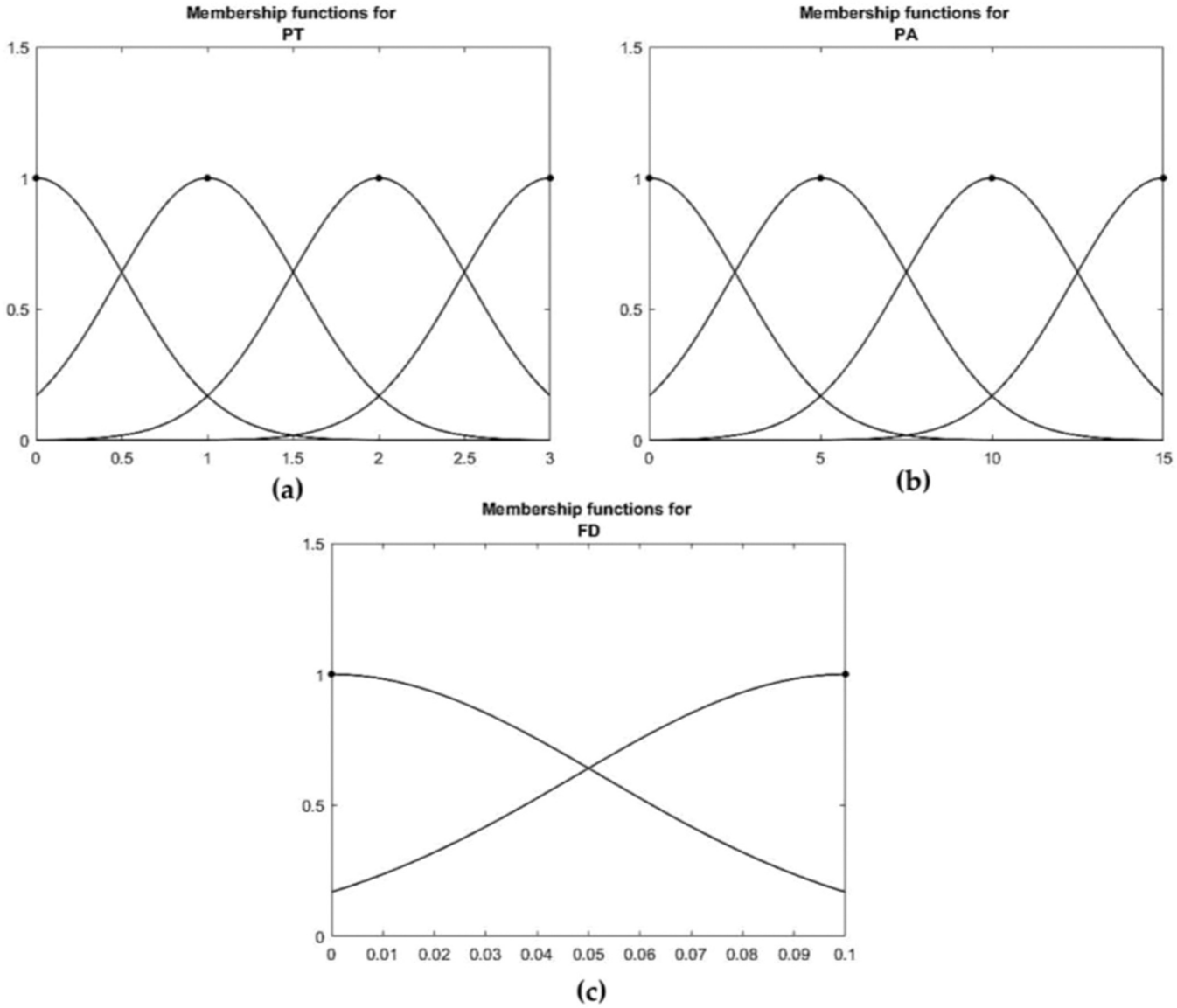

Fig. 11. Membership functions for three inputs **(a)** pozzolan type (PT), **(b)** pozzolan amount (PA), and **(c)** fiber dosage (FD).

modeling the repair layer. One key benefit is its flexibility in allowing the creation of models with specific dimensions that closely replicate real-world applications.

3.2. Prediction of Shear Bond Strength

In this study, the factors identified as significantly impacting the bond strength of FRSCC are the type and amount of pozzolan, and the dosage of fibers. These variables have been selected for the prediction of shear bond strength.

3.2.1. Generalized Mamdani fuzzy system

For the purpose of predicting shear bond strength, the fuzzy system delineated in Eq. (6) is employed in conjunction with a generalized Mamdani's inference engine, characterized by the Frank family of t-norms as detailed in Eq. (7):

$$\varphi(x,y) = T_F^s(x,y) = \log_s\left(1 + \frac{(s^x - 1)(s^y - 1)}{s - 1}\right) \tag{7}$$

Here, $s > 0$ and $s \neq 1$. In addition, the system utilizes a singleton fuzzifier and a centre average defuzzifier, as outlined in Eqs. (8) and (9), respectively. The input variables, namely pozzolan type, pozzolan amount, and fibre dosage, are characterized using Gaussian membership functions, as depicted in Fig. 11a-c:

$$\mu_{A'}(t) = \begin{cases} 1 & t = x \\ 0 & \text{otherwise} \end{cases} \tag{8}$$

$$y^* = \frac{\sum_{l=1}^{M} \bar{y}^l w_l}{\sum_{l=1}^{M} w_l} \tag{9}$$

where $y^* \in U$; $\bar{y}^l$ is the centre of the l 's individual output fuzzy set $\bar{B}^l$; and w_l is its height.

Fig. 12 a-h present a comparative analysis between the shear bond strength values calculated using the proposed fuzzy method and those obtained from experimental tests. The results showcased in Fig. 6a-h demonstrate that the proposed fuzzy system, in conjunction with the Frank family of t-norms, accurately predicts the shear bond strength. Notably, the most precise predictions were achieved with different t-norms, as evidenced by the coefficient of determination (R^2) values: $T_F^{0.5}$ (R^2=0.94048 in Fig. 12a), T_F^2 (R^2=0.94959 in Fig. 12b), T_F^5 (R^2=0.95347 in Fig. 12c), T_F^{10} (R^2=0.9555 in Fig. 12d), T_F^{100} (R^2=0.95882 in Fig. 12e), T_F^{1000} (R^2=0.95971 in Fig. 12f), $T_F^{1,000,000}$ (R^2=0.95997 in Fig. 12g) and

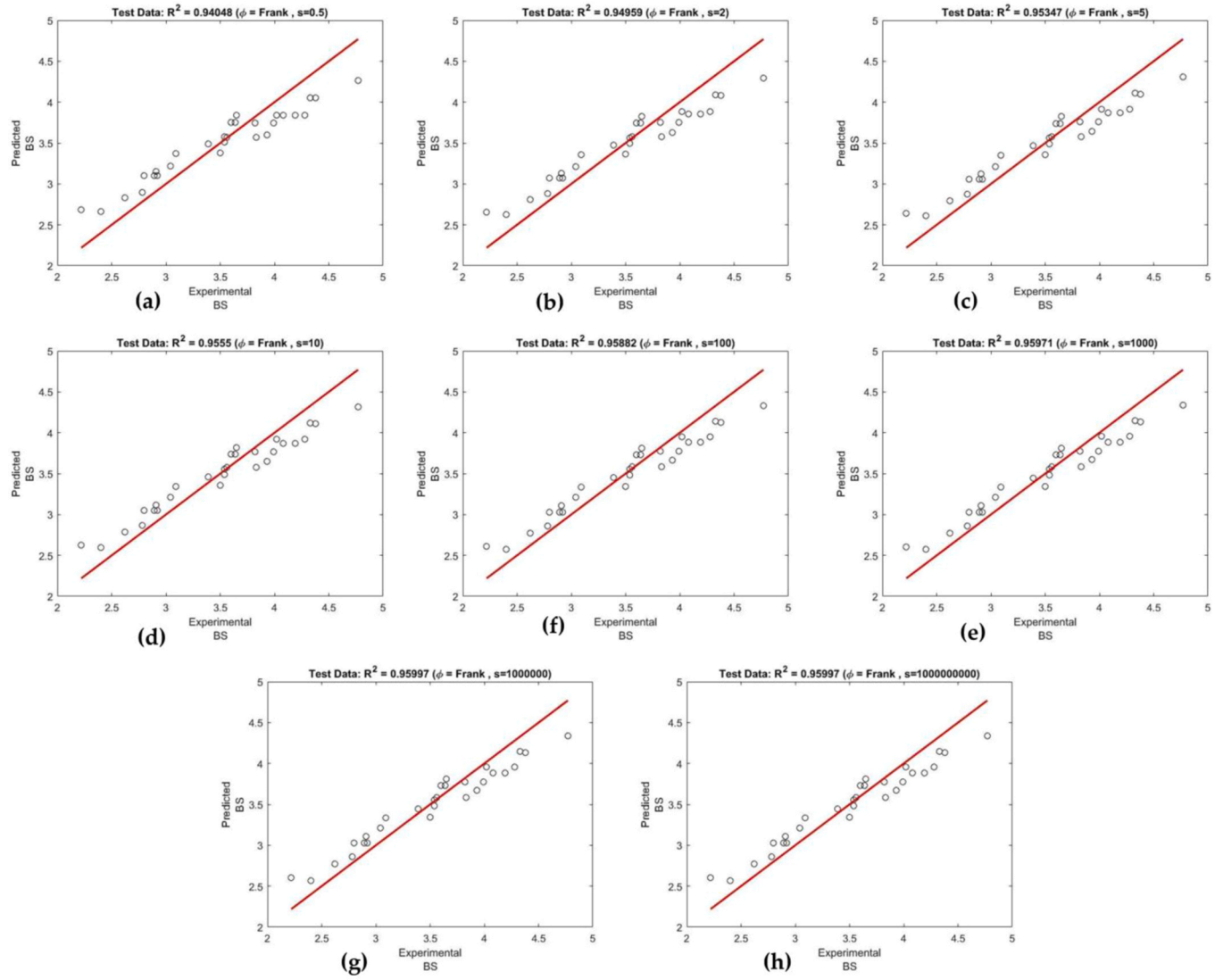

Fig. 12. Prediction of bond strength with proposed fuzzy logic inference system using Frank family of t-norms: (a) s = 0.5, (b) s = 2, (c) s = 5, (d) s = 10, (e) s = 100, (f) s = 1000, (g) s = 1000000, and (h) s = 1000000000.

$T_F^{1,000,000,000}$ (R^2=0.95997 in Fig. 12h).

3.2.2. Linear Regression

In an effort to predict shear bond strength (BS), a linear regression model culminates in the formulation of Eq. (10):

$$BS = 1.570 + 0.201\ PT - 0.006\ PA + 3.670\ FD \quad (10)$$

In this equation, *PT* represents the type of pozzolan (where *PT*=0 indicates no pozzolan, *PT*=1 for zeolite, *PT*=2 for slag, and *PT*=3 for micro silica), *PA* denotes the amount of pozzolan in percent, and *FD* refers to the fiber dosage in percent.

Fig. 13 displays a comparison between the shear bond strength values obtained from experimental tests and those calculated using Eq. (10). It can be observed that the R^2 values is equal to 0.8456. This outcome suggests that the predictions made by the proposed fuzzy system are more precise compared to those from the linear regression model. Furthermore, the adaptability of the proposed fuzzy system is such that it can be extended to calculate the shear bond strength of other FRSCC mixes, showcasing its versatility and applicability in a broader context.

The findings of this study lead to the conclusion that employing fuzzy systems with a generalized Mamdani's inference engine, as defined by the Frank family of t-norms, is an effective method for predicting shear bond strength. However, it is essential to note that the fuzzy system was trained using a limited number of FRSCC mixes and only one type of fiber. Consequently, further research is necessary to broaden the scope of the system's application. This would involve extending its capacity to accurately predict shear bond strength for a broader range of FRSCC mixes that incorporate various other types of fibers.

4. Conclusions

This study provided a comprehensive examination of shear bond strength in FRSCC, utilizing twenty distinct mix formulations. The research focused on analyzing the impact of three types of pozzolans – microsilica, zeolite, and slag – incorporated at various concentrations relative to cement weight, along with the assessment of polypropylene fibers at 0 and 0.1% volume dosages. The investigation had two primary objectives:

1) To evaluate the push-out test as a feasible alternative to the slant shear test for determining shear bond strength in FRSCC.
2) To implement and validate a fuzzy logic-based predictive modeling approach, employing a generalized Mamdani model with the Frank family of t-norms, for accurate prediction of FRSCC's shear bond strength.

The key conclusions drawn from this study are as follows:

- Fiber inclusion slightly lowers SCC workability, yet microsilica's use in FRSCC offsets this, underscoring the need for meticulous mix design to preserve self-compacting qualities and enhance mechanical performance.
- It is discerned from the analysis that fibers primarily serve functions beyond augmenting compressive strength, whereas the inclusion of pozzolans—particularly microsilica at a 10% ratio—plays a pivotal role in elevating the compressive strength metrics of SCC.
- Enhanced tensile strengths in FRSCC are attributed to fibers, with 15% microsilica and slag markedly amplifying this effect, demonstrating the importance of pozzolan selection for optimal fiber synergy.
- A strong correlation between push-out and slant shear test results (R^2 = 0.88) underscores the push-out test's potential as a practical and efficient alternative for bond strength assessment.
- The study underscores fiber inclusion's impact on FRSCC bond strength, with 15% microsilica and slag providing significant benefits, whereas zeolite's effect is less consistent.
- The fuzzy logic approach successfully predicted shear bond strength with high accuracy (R^2 up to 0.95997), validating the model's effectiveness.

While this research successfully establishes the push-out test as an effective evaluation tool for shear bond strength and introduces a robust fuzzy system model for prediction, it acknowledges the limitations, such as the limited training data for the fuzzy logic model, the constrained range of FRSCC mixes and fiber types examined. Future research should aim to include providing more experimental data to create a more reliable fuzzy logic model, a broader array of mix compositions and diverse fiber types, as expanding the scope of the study is crucial for fully validating the general applicability and reliability of the proposed methodologies. In conclusion, this research significantly contributes to concrete technology, offering new insights and methodologies for enhanced structural assessment and material optimization in FRSCC. By integrating practical testing methods with advanced predictive modeling, this study not only furthers the understanding of fiber-

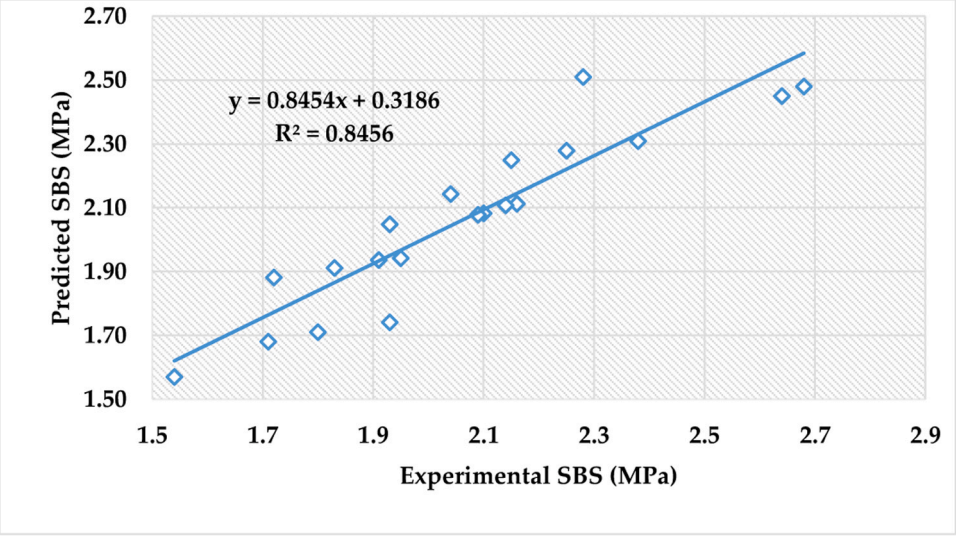

Fig. 13. Comparison of predicted SBS values with experimental results.

reinforced concrete structures but also sets the stage for future innovations in concrete technology.

Funding

This research received no external funding.

CRediT authorship contribution statement

Raffaele Cucuzza: Writing – review & editing, Visualization, Supervision, Investigation. **Majid Movahedi Rad:** Writing – review & editing, Validation, Supervision. **Amin Ghodousian:** Validation, Software, Methodology. **Vahid Shafaie:** Writing – original draft, Visualization, Resources, Investigation, Formal analysis. **Oveys Ghodousian:** Writing – review & editing, Validation, Supervision, Resources, Methodology, Conceptualization.

Declaration of Competing Interest

The authors declare that they have no known competing financial interests or personal relationships that could have appeared to influence the work reported in this paper.

Data Availability

No data was used for the research described in the article.

Acknowledgements

The authors would like to acknowledge the support of those who directly or indirectly contributed to the success of this study.

References

[1] A.D. Espeche, J. León, Estimation of bond strength envelopes for old-to-new concrete interfaces based on a cylinder splitting test, Constr. Build. Mater. 25 (2011) 1222–1235, https://doi.org/10.1016/j.conbuildmat.2010.09.032.
[2] O. Ghodousian, R. Garcia, V. Shafaie, A. Ghodousian, Interfacial bond strength of coloured SCC repair layers: an experimental and optimisation study, J. Struct. Integr. Maint. 00 (2023) 1–10, https://doi.org/10.1080/24705314.2023.2170620.
[3] M. Eymard, J.-P. Plassiard, P. Perrotin, S. Le Fay, Interfacial strength study between a concrete substrate and an innovative sprayed coating, Constr. Build. Mater. 79 (2015) 345–356, https://doi.org/10.1016/j.conbuildmat.2014.12.031.
[4] E.N.B.S. Júlio, F.A.B. Branco, V.D. Silva, Concrete-to-concrete bond strength. Influence of the roughness of the substrate surface, Constr. Build. Mater. 18 (2004) 675–681, https://doi.org/10.1016/j.conbuildmat.2004.04.023.
[5] E.N.B.S. Júlio, F.A.B. Branco, V.D. Silva, Concrete-to-concrete bond strength: influence of an epoxy-based bonding agent on a roughened substrate surface, Mag. Concr. Res. 57 (2005) 463–468, https://doi.org/10.1680/macr.2005.57.8.463.
[6] P.M.D. Santos, E.N.B.S. Júlio, Factors Affecting Bond between New and Old Concrete, Acids Mater. J. 108 (2011) 449–456. ⟨https://api.semanticscholar.org/CorpusID:137674943⟩.
[7] R. Mirmoghtadaei, M. Mohammadi, N. Ashraf Samani, S. Mousavi, The impact of surface preparation on the bond strength of repaired concrete by metakaolin containing concrete, Constr. Build. Mater. 80 (2015) 76–83, https://doi.org/10.1016/j.conbuildmat.2015.01.018.
[8] D.P. Bentz, I. De la Varga, J.F. Muñoz, R.P. Spragg, B.A. Graybeal, D.S. Hussey, D. L. Jacobson, S.Z. Jones, J.M. LaManna, Influence of substrate moisture state and roughness on interface microstructure and bond strength: Slant shear vs. pull-off testing, Cem. Concr. Compos. 87 (2018) 63–72, https://doi.org/10.1016/j.cemconcomp.2017.12.005.
[9] P.M.D. Santos, E.N.B.S. Júlio, V.D. Silva, Correlation between concrete-to-concrete bond strength and the roughness of the substrate surface, Constr. Build. Mater. 21 (2007) 1688–1695, https://doi.org/10.1016/j.conbuildmat.2006.05.044.
[10] Y. He, X. Zhang, R.D. Hooton, X. Zhang, Effects of interface roughness and interface adhesion on new-to-old concrete bonding, Constr. Build. Mater. 151 (2017) 582–590, https://doi.org/10.1016/j.conbuildmat.2017.05.049.
[11] E.N.B.S. Júlio, F.A.B. Branco, V.D. Silva, J.F. Lourenço, Influence of added concrete compressive strength on adhesion to an existing concrete substrate, Build. Environ. 41 (2006) 1934–1939, https://doi.org/10.1016/j.buildenv.2005.06.023.
[12] M. Naderi, O. Ghodousian, Adhesion of self-compacting overlays applied to different concrete substrates and its prediction by fuzzy logic, J. Adhes. 88 (2012) 848–865, https://doi.org/10.1080/00218464.2012.705673.
[13] M.A. Issa, R.Z. Alrousan, High performance bonded concrete overlays, in: Int. Conf. Constr. Build. Technol. ICCBT 2008-(01), 2008: pp. 1–20.
[14] C. Zanotti, N. Randl, Are concrete-concrete bond tests comparable? Cem. Concr. Compos. 99 (2019) 80–88, https://doi.org/10.1016/j.cemconcomp.2019.02.012.
[15] Y. Zhang, P. Zhu, Z. Liao, L. Wang, Interfacial bond properties between normal strength concrete substrate and ultra-high performance concrete as a repair material, Constr. Build. Mater. 235 (2020) 117431, https://doi.org/10.1016/j.conbuildmat.2019.117431.
[16] A. Momayez, M.R. Ehsani, A.A. Ramezanianpour, H. Rajaie, Comparison of methods for evaluating bond strength between concrete substrate and repair materials, Cem. Concr. Res. 35 (2005) 748–757, https://doi.org/10.1016/j.cemconres.2004.05.027.
[17] A. Sademomtazi, O. Ghodousian, Study of effect of freezing and thawing cycles on bonding between fiber-reinforced self-compacting concrete with different water to cementitious ratios and paste volume as a repair layer and concrete substrate, MCEJ (Persian) 18 (2018) 129–139. ⟨http://mcej.modares.ac.ir/article-16-15719-en.html⟩.
[18] A. Sademomtazi, O. Ghodousian, Comparison of pull-off, push-out and splitting prism tests for assessment of bonding between fiber-reinforced self-compacting concrete as a repair layer and concrete substrate, J. Struct. Constr. Eng. (Persian). 6 (2018) 199–212, https://doi.org/10.22065/jsce.2018.106322.1388.
[19] A.M. Diab, A.E.M. Abd Elmoaty, M.R. Tag Eldin, Slant shear bond strength between self compacting concrete and old concrete, Constr. Build. Mater. 130 (2017) 73–82, https://doi.org/10.1016/j.conbuildmat.2016.11.023.
[20] Z. Dawei, U. Tamon, F. Hitoshi, Average Crack Spacing of Overlay-Strengthened RC Beams, J. Mater. Civ. Eng. 23 (2011) 1460–1472, https://doi.org/10.1061/(ASCE)MT.1943-5533.0000316.
[21] N. Banthia, R. Gupta, S. Mindess, Development of fiber reinforced concrete repair materials, Can. J. Civ. Eng. 33 (2006) 126–133, https://doi.org/10.1139/l05-093.
[22] R. Cucuzza, M. Domaneschi, G. Camata, G.C. Marano, A. Formisano, D. Brigante, FRCM retrofitting techniques for masonry walls: a literature review and some laboratory tests, Procedia Struct. Integr. 44 (2022) 2190–2197, https://doi.org/10.1016/j.prostr.2023.01.280.
[23] R. Cucuzza, A. Aloisio, F. Accornero, A. Marinelli, E. Bassoli, G.C. Marano, Size-scale effects and modelling issues of fibre-reinforced concrete beams, Constr. Build. Mater. 392 (2023) 131727, https://doi.org/10.1016/j.conbuildmat.2023.131727.
[24] S. Khaleel Ibrahim, N. Abbas Hadi, M. Movahedi Rad, Experimental and Numerical Analysis of Steel-Polypropylene Hybrid Fibre Reinforced Concrete Deep Beams, Polym. (Basel) 15 (2023), https://doi.org/10.3390/polym15102340.
[25] S. Khaleel Ibrahim, M. Movahedi Rad, Limited optimal plastic behavior of RC beams strengthened by carbon fiber polymers using reliability-based design, Polymers 15 (2023), https://doi.org/10.3390/polym15030569.
[26] A. Sadrmomtazi, O. Ghodousian, Study of effect of paste volume, water to cementitious materials and fiber dosages onrheological properties and in-situ strength of self- compacting concrete, J. Rehabil. Civ. Eng. 7 (2019) 68–79, https://doi.org/10.22075/JRCE.2018.13057.1236.
[27] A. Albidah, A. Abadel, F. Alrshoudi, A. Altheeb, H. Abbas, Y. Al-Salloum, Bond strength between concrete substrate and metakaolin geopolymer repair mortars at ambient and elevated temperatures, J. Mater. Res. Technol. 9 (2020) 10732–10745, https://doi.org/10.1016/j.jmrt.2020.07.092.
[28] B.A. Tayeh, B.H. Abu Bakar, M.A. Megat Johari, Y.L. Voo, Mechanical and permeability properties of the interface between normal concrete substrate and ultra high performance fiber concrete overlay, Constr. Build. Mater. 36 (2012) 538–548, https://doi.org/10.1016/j.conbuildmat.2012.06.013.
[29] S. Jafarinejad, A. Rabiee, M. Shekarchi, Experimental investigation on the bond strength between ultra high strength fiber reinforced cementitious mortar & conventional concrete, Constr. Build. Mater. 229 (2019) 116814, https://doi.org/10.1016/j.conbuildmat.2019.116814.
[30] C. Zanotti, G. Rostagno, B. Tingley, Further evidence of interfacial adhesive bond strength enhancement through fiber reinforcement in repairs, Constr. Build. Mater. 160 (2018) 775–785, https://doi.org/10.1016/j.conbuildmat.2017.12.140.
[31] C. Zanotti, N. Banthia, G. Plizzari, A study of some factors affecting bond in cementitious fiber reinforced repairs, Cem. Concr. Res. 63 (2014) 117–126, https://doi.org/10.1016/j.cemconres.2014.05.008.
[32] A. Turatsinze, J.-L. Granju, V. Sabathier, H. Farhat, Durability of bonded cement-based overlays: effect of metal fibre reinforcement, Mater. Struct. 38 (2005) 321–327, https://doi.org/10.1007/BF02479297.
[33] J. Zhang, H. Stang, V.C. Li, Crack bridging model for fibre reinforced concrete under fatigue tension, Int. J. Fatigue 23 (2001) 655–670, https://doi.org/10.1016/S0142-1123(01)00041-X.
[34] P. Rossi, Le développement industriel des bé-tons de fibres métalliques – Conclusions et re-commandations, Press. l'École Natl. Ponts Chaussées, (In French). (2002).
[35] S. Feng, H. Xiao, Y. Li, Influence of interfacial parameters and testing methods on UHPC–NSC bond strength: Slant shear vs. direct tensile testing, Cem. Concr. Compos. 131 (2022) 104568, https://doi.org/10.1016/j.cemconcomp.2022.104568.
[36] B. Hu, Y. Li, Y. Liu, Dynamic slant shear bond behavior between new and old concrete, Constr. Build. Mater. 238 (2020) 117779, https://doi.org/10.1016/j.conbuildmat.2019.117779.
[37] R. Saldanha, E. Júlio, D. Dias-da-Costa, P. Santos, A modified slant shear test designed to enforce adhesive failure, Constr. Build. Mater. 41 (2013) 673–680, https://doi.org/10.1016/j.conbuildmat.2012.12.053.
[38] S. Feng, H. Xiao, H. Li, Comparative studies of the effect of ultrahigh-performance concrete and normal concrete as repair materials on interfacial bond properties and microstructure, Eng. Struct. 222 (2020) 111122, https://doi.org/10.1016/j.engstruct.2020.111122.

[39] S. Feng, H. Xiao, J. Geng, Bond strength between concrete substrate and repair mortar: Effect of fibre stiffness and substrate surface roughness, Cem. Concr. Compos. 114 (2020) 103746, https://doi.org/10.1016/j.cemconcomp.2020.103746.
[40] Q. Luo, W. Wang, B. Wang, S. Xu, Z. Sun, Numerical study on interface optimization of new-to-old concrete with the slant grooves, Structures 34 (2021) 381–399, https://doi.org/10.1016/j.istruc.2021.07.094.
[41] O. Ghodousian, A. Ghodousian, V. Shafaie, S. Hajiloo, M. Movahedi Rad, Study of Bonding between Façade Stones and Substrates with and without Anchorage Using Shear-Splitting Test—Case Study: Travertine, Granite, and Marble, Buildings 13 (2023), https://doi.org/10.3390/buildings13051229.
[42] V.W.Y. Tam, A. Butera, K.N. Le, L.C.F.Da Silva, A.C.J. Evangelista, A prediction model for compressive strength of CO2 concrete using regression analysis and artificial neural networks, Constr. Build. Mater. 324 (2022) 126689, https://doi.org/10.1016/j.conbuildmat.2022.126689.
[43] A.A. Shahmansouri, M. Yazdani, M. Hosseini, H. Akbarzadeh Bengar, H. Farrokh Ghatte, The prediction analysis of compressive strength and electrical resistivity of environmentally friendly concrete incorporating natural zeolite using artificial neural network, Constr. Build. Mater. 317 (2022) 125876, https://doi.org/10.1016/j.conbuildmat.2021.125876.
[44] E.M. Golafshani, A. Rahai, M.H. Sebt, H. Akbarpour, Prediction of bond strength of spliced steel bars in concrete using artificial neural network and fuzzy logic, Constr. Build. Mater. 36 (2012) 411–418, https://doi.org/10.1016/j.conbuildmat.2012.04.046.
[45] M. Sarıdemir, İ.B. Topçu, F. Özcan, M.H. Severcan, Prediction of long-term effects of GGBFS on compressive strength of concrete by artificial neural networks and fuzzy logic, Constr. Build. Mater. 23 (2009) 1279–1286, https://doi.org/10.1016/j.conbuildmat.2008.07.021.
[46] İ.B. Topçu, M. Sarıdemir, Prediction of compressive strength of concrete containing fly ash using artificial neural networks and fuzzy logic, Comput. Mater. Sci. 41 (2008) 305–311, https://doi.org/10.1016/j.commatsci.2007.04.009.
[47] İ.B. Topçu, M. Sarıdemir, Prediction of mechanical properties of recycled aggregate concretes containing silica fume using artificial neural networks and fuzzy logic, Comput. Mater. Sci. 42 (2008) 74–82, https://doi.org/10.1016/j.commatsci.2007.06.011.
[48] İ.B. Topçu, M. Sarıdemir, Prediction of rubberized concrete properties using artificial neural network and fuzzy logic, Constr. Build. Mater. 22 (2008) 532–540, https://doi.org/10.1016/j.conbuildmat.2006.11.007.
[49] A.A. Shahmansouri, H. Akbarzadeh Bengar, E. Jahani, Predicting compressive strength and electrical resistivity of eco-friendly concrete containing natural zeolite via GEP algorithm, Constr. Build. Mater. 229 (2019) 116883, https://doi.org/10.1016/j.conbuildmat.2019.116883.
[50] H. Tanyildizi, Fuzzy logic model for the prediction of bond strength of high-strength lightweight concrete, Adv. Eng. Softw. 40 (2009) 161–169, https://doi.org/10.1016/j.advengsoft.2007.05.013.
[51] H. Tanyildizi, Fuzzy logic model for prediction of mechanical properties of lightweight concrete exposed to high temperature, Mater. Des. 30 (2009) 2205–2210, https://doi.org/10.1016/j.matdes.2008.08.030.
[52] F. Demir, A new way of prediction elastic modulus of normal and high strength concrete—fuzzy logic, Cem. Concr. Res. 35 (2005) 1531–1538, https://doi.org/10.1016/j.cemconres.2005.01.001.
[53] O. Ghodousian, R. Garcia, A. Ghodousian, M.H. Mohammad Nezhad Ayandeh, Properties of fibre-reinforced self-compacting concrete subjected to prolonged mixing: an experimental and fuzzy logic investigation, J. Build. Pathol. Rehabil. 9 (2024) 22, https://doi.org/10.1007/s41024-023-00374-3.
[54] O. Ghodousian, K. Behdad, V. Shafaie, A. Ghodousian, H. Mehdikhani, Predicting 28-day compressive strength of pozzolanic concrete by generalized nearest neighborhood clustering using modified pso algorithm, Malays. Constr. Res. J. 33 (2021) 61–72.
[55] W.R.L. da Silva, P. Stemberk, Genetic-fuzzy approach to model concrete shrinkage, Comput. Concr. 12 (2013) 109–129, https://doi.org/10.12989/CAC.2013.12.2.109.
[56] M.E. Arslan, A. Durmus, Fuzzy logic approach for estimating bond behavior of lightweight concrete, Comput. Concr. 14 (2014) 233–245, https://doi.org/10.12989/CAC.2014.14.3.233.
[57] M.F. Najjar, M.L. Nehdi, T.M. Azabi, A.M. Soliman, Fuzzy inference systems based prediction of engineering properties of two-stage concrete, Comput. Concr. 19 (2017) 133–142, https://doi.org/10.12989/CAC.2017.19.2.133.
[58] K. Rashid, T. Rashid, Fuzzy logic model for the prediction of concrete compressive strength by incorporating green foundry sand, Comput. Concr. 19 (2017) 617–623, https://doi.org/10.12989/CAC.2017.19.6.617.
[59] A. Beycioglu, A. Gultekin, H.Y. Aruntas, O. Gencel, M. Dobiszewska, W. Brostow, Mechanical properties of blended cements at elevated temperatures predicted using a fuzzy logic model, Comput. Concr. 20 (2017) 247–255, https://doi.org/10.12989/CAC.2017.20.2.247.
[60] M. Gencoglu, T. Uygunoglu, F. Demir, K. Guler, Prediction of elastic modulus of steel-fiber reinforced concrete (SFRC) using fuzzy logic, Comput. Concr. 9 (2012) 389–402, https://doi.org/10.12989/CAC.2012.9.5.389.
[61] ASTM C33/C33M-18, Standard Specification for Concrete Aggregates, West Conshohocken, PA, 2018. https://doi.org/10.1520/C0033_C0033M-18.
[62] A.M. Saba, A.H. Khan, M.N. Akhtar, N.A. Khan, S.S. Rahimian Koloor, M. Petrů, N. Radwan, Strength and flexural behavior of steel fiber and silica fume incorporated self-compacting concrete, J. Mater. Res. Technol. 12 (2021) 1380–1390, https://doi.org/10.1016/j.jmrt.2021.03.066.
[63] S.Y. Ghanem, J. Bowling, Z. Sun, Mechanical Properties of Hybrid Synthetic Fiber Reinforced Self- Consolidating Concrete, Compos. Part C. Open Access. 5 (2021) 100154, https://doi.org/10.1016/j.jcomc.2021.100154.
[64] EFNARC, The European Guidelines for Self-compacting Concrete. Specification, Production and Use, 2005.
[65] L.N. Thrane, C.V. Nielsen, C. Pade, Guidelines for Execution of SCC, Danish Technol. Institute, Concr. Cent. Taastrup, Denmark. (2008).
[66] C. Pade, L.N. Thrane, C.V. Nielson, Guidelines for Mix Design of SCC, Danish Technol. Institute, Concr. Cent. Taastrup, Denmark. (2008).
[67] ASTM C39/C39M-23, Standard Test Method for Compressive Strength of Cylindrical Concrete Specimens, Am. Soc. Test. Mater. Pennsylvania, USA. (2023).